







# Study on Characteristics of Coupled-Core Four-Core Fibers With Different Core Pitches

Junjie Xiong , Lin Ma , Senior Member, IEEE, Yanming Chang , Tianqi Cheng, Lei Shen, Lei Zhang, Changkun Yan, Lin Sun , Member, IEEE, Qingwen Liu , Member, IEEE, and Zuyuan He , Senior Member, IEEE, Senior Member, OSA

**Abstract**—We studied the characteristics of coupled-core four-core fibers (CC-4CFs) with different core pitches both theoretically and experimentally. The spatial mode dispersions of different fibers were analyzed, and the result agrees well with theoretical ones. In the experiment, we achieved a spatial mode dispersion as low as 3.72 ps/km<sup>1/2</sup> for a 4 km-long CC-4CF with core pitch of 19 μm at a bending radius of 8 cm. The impulse response matrices of four core fibers with different core pitches was investigated using swept-wavelength interferometry over 100 nm bandwidth. The impulse responses were Gaussian-shaped and consistent between different inputs and outputs for CC-4CFs. Our results show that the CC-4CFs with core pitches of 17 and 19 μm exhibit narrower pulse broadening. In addition, the mode-dependent losses of different fibers were analyzed. For the fibers with core pitch of 19 μm, the estimated mode-dependent loss was lower than 3 dB for the entire 100 nm bandwidth. Our results are especially helpful for developing coupled-core multicore fibers for long-haul transmission applications.

**Index Terms**—Coupled-core multicore fiber, impulse response, spatial mode dispersion, swept-wavelength interferometry, transfer matrix.

## I. INTRODUCTION

MULTICORE fibers (MCFs) have been considered to be promising candidates to overcome the upcoming capacity crunch of traditional fiber transmission systems [1], [2], [3]. They can be divided into weakly-coupled MCF (WC-MCF) and coupled-core MCF (CC-MCF). For WC-MCFs, cores are used as independent channels for data transmissions [4]. The core pitch of this type is sufficiently large to suppress the inter-core

crosstalk. On the other hand, the core pitch of CC-MCF is relatively small to introduce random mode coupling, which has distinctive advantages such as reduced spatial mode dispersion (SMD) [5], lower mode-dependent loss (MDL) [6], and mitigation of nonlinear effect [7]. Several transmission experiments have shown that CC-MCFs are promising fibers from the point of view of both system architecture design and applicability for long-haul transmission using multiple-input-multiple-output (MIMO) digital signal processing (DSP) technology [8], [9], [10].

SMD and MDL are important characteristics of CC-MCFs. Reduced SMD can effectively reduce the MIMO DSP complexity [11]. MDL leads to the difference in the mode optical signal-to-noise ratio (OSNR), which results in non-unitary channel transfer matrix and then cause the degradation of MIMO DSP [12]. The SMD and MDL mainly rely on the mode coupling between cores and external perturbation like fiber twisting and bending [13]. Mode coupling characteristics are susceptible to many factors like core pitch, index profile, and core arrangement, of which the core pitch has a more direct and significant effect [14], [15]. As a result, core pitch design optimization is crucial for the design of CC-MCFs.

In recent years, the 125 μm-cladding MCFs have been studied extensively due to their good reliability and compatibility with standard single-mode fiber (SSMF) facilities. The CC-MCFs with 125 μm cladding have also received wide attention and have been deployed and tested in the field [16]. There are some numerical studies about the SMD and mode coupling of CC-MCFs [17]. The SMD analysis of different coupled-core two-core fibers with homogeneous and heterogenous cores has been studied [18]. And the comparison between transfer matrices of coupled-core four-core fiber (CC-4CF) and weakly-coupled four-core fiber (WC-4CF) has been proposed [19]. However, the SMDs and transfer matrices of CC-4CFs with different core pitches have not been experimentally studied and analyzed yet.

In this article, we experimentally investigated the dependence of SMD and transfer matrix on core pitch of CC-4CFs for the first time to the best of our knowledge. Distinguishable differential group delay (DGD) distribution can be observed for CC-4CFs with different core pitches, and the measured SMDs agreed well with the calculated ones. In our experiment, the lowest SMD coefficient of 3.72 ps/km<sup>1/2</sup> was achieved for a 4 km-long CC-4CF with core pitch of 19 μm, which is the lowest SMD ever reported when the fibers under test were wound

Manuscript received 18 October 2023; revised 1 December 2023; accepted 5 December 2023. Date of publication 12 December 2023; date of current version 26 December 2023. This work was supported in part by the National Key R&D Program of China under Grant 2018YFB1801000 and in part by the National Natural Science Foundation of China (NSFC) under Grants 62275150 and 61835006. (Corresponding author: Lin Ma.)

Junjie Xiong, Lin Ma, Yanming Chang, Tianqi Cheng, Qingwen Liu, and Zuyuan He are with the State Key Laboratory of Advanced Optical Communication Systems and Networks, Shanghai Jiao Tong University, Shanghai 200240, China (e-mail: xiongjunjie@sjtu.edu.cn; ma.lin@sjtu.edu.cn; changyanming@sjtu.edu.cn; tianqi.cheng@sjtu.edu.cn; liuqingwen@sjtu.edu.cn; zuyuanhe@sjtu.edu.cn).

Lei Shen, Lei Zhang, and Changkun Yan are with the State Key Laboratory of Optical Fiber and Cable Manufacture Technology, Yangtze Optical Fiber and Cable Joint Stock Limited Company, Wuhan 430073, China (e-mail: shenlei@yofc.com; zhanglei@yofc.com; yanckun@yofc.com).

Lin Sun is with the Suzhou Key Laboratory of Advanced Optical Communication Network Technology, School of Electronic and Information Engineering, Soochow University, Suzhou 215006, China (e-mail: linsun@suda.edu.cn).

Digital Object Identifier 10.1109/JPHOT.2023.3341415

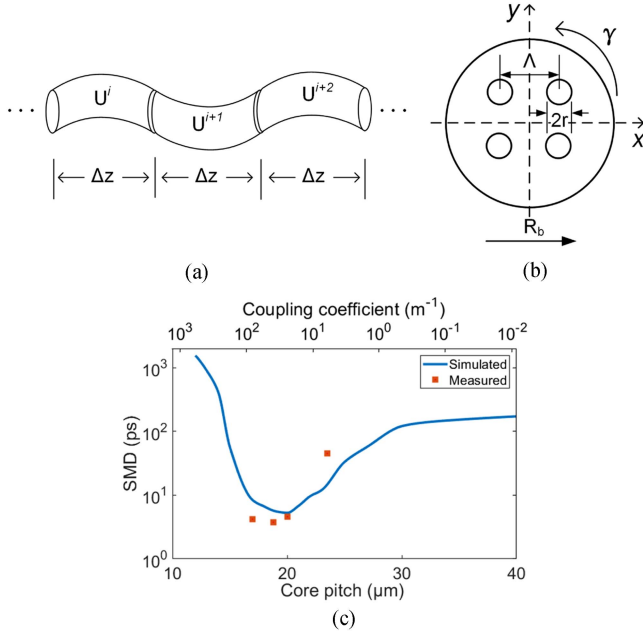


Fig. 1. (a) Fiber modeling by the concatenation of segments. (b) Schematic of the four-core fiber with bending and twisting. (c) Calculated (blue line) and measured (red square) SMD after 1 km propagation for different core pitches.

on the standard 8 cm-radius bobbins. The impulse response matrices of four core fibers with different core pitches were also investigated using swept-wavelength interferometry (SWI) over 100 nm bandwidth. The MDLs of different fibers were estimated from the measured transfer matrices, and it was lower than 3 dB for the CC-4CF with a core pitch of 19  $\mu\text{m}$  over the entire 100 nm bandwidth. The presented studies give a detailed investigation for the impact of the core pitch on the performance of multicore fibers and are beneficial for developing coupled-core multicore fibers for long-haul transmission applications.

## II. FIBER DESIGN AND FABRICATION

We employed a coupled mode theory to study the mode coupling effect and SMD of the CC-4CFs [20], [21], which can be expressed as

$$\frac{dA_l(z)}{dz} = -j\beta_l A_l(z) + j \sum_{m \neq l} \kappa_{lm} A_m(z), \quad (1)$$

where  $A_l(z)$  and  $A_m(z)$  are the complex field amplitudes, and  $\beta_l$  is the propagation constant of the core  $l$ . The  $\kappa_{lm}$  represents the coupling coefficient between the core  $l$  and core  $m$ , which is calculated by [22]

$$\kappa_{lm} = \omega \varepsilon_0 \frac{\int_{-\infty}^{+\infty} \int_{-\infty}^{+\infty} (N^2 - N_m^2) \mathbf{E}_l^* \cdot \mathbf{E}_m dx dy}{\int_{-\infty}^{+\infty} \int_{-\infty}^{+\infty} \mathbf{u}_z \cdot (\mathbf{E}_l^* \times \mathbf{H}_l + \mathbf{E}_l \times \mathbf{H}_l^*) dx dy}, \quad (2)$$

where  $\omega$  is the angular frequency of electromagnetic field,  $\varepsilon_0$  is the permittivity in the vacuum.  $\mathbf{E}_l$  and  $\mathbf{E}_m$  represent the electric field distribution in core  $l$  and core  $m$ . The fiber was modeled as a concatenation of many segments, as shown in Fig. 1(a). The length of the segment is set to be small enough so that the fiber

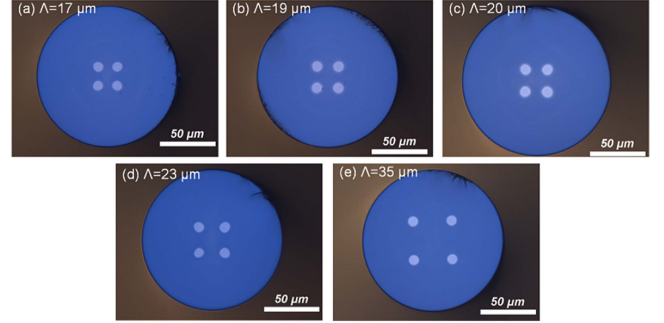


Fig. 2. Cross-sectional micrographs of fabricated 4CFs with core pitches of about (a) 17  $\mu\text{m}$ , (b) 19  $\mu\text{m}$ , (c) 20  $\mu\text{m}$ , (d) 23  $\mu\text{m}$ , and (e) 35  $\mu\text{m}$ .

in each segment can be assumed to be uniform. In each segment, the solution of (1) can be expressed as

$$\mathbf{A}(z + \Delta z) = \mathbf{U}^i(\omega) \cdot \mathbf{A}(z), \quad (3)$$

where  $\mathbf{A}(z) = [A_1(z); A_2(z); \dots; A_n(z)]$  is a column vector of the field amplitude.  $\mathbf{U}^i(\omega)$  is the transmission matrix of  $i$ -th segment. And the total transmission matrix of the fiber is given by

$$\mathbf{U}^{tot}(\omega) = \prod_{i=1}^N \mathbf{U}^i(\omega), \quad (4)$$

where  $N$  is the total number of segments. The group delay operator  $\mathbf{GDO}(\omega)$  is defined as [23]

$$\mathbf{GDO}(\omega) = -j(\mathbf{U}^{tot}(\omega))^{-1} \frac{d\mathbf{U}^{tot}(\omega)}{d\omega}. \quad (5)$$

The SMD of the fiber is given by

$$SMD = \sqrt{\frac{1}{n} \sum_{i=1}^n \tau_i^2}, \quad (6)$$

where  $n$  is the total number of modes, and  $\tau_i$  is the  $i$ -th eigenvalue of the  $\mathbf{GDO}(\omega)$ .

In our calculation, a typical single-mode fiber core design ( $r = 4.5 \mu\text{m}$ ,  $\Delta = 0.37\%$ ) was adopted for the CC-4CFs, and a core radius difference of  $\pm 1\%$  was used to assume the inter-core differences introduced during the drawing process. The random coupling was considered by fiber bending and twisting, as shown in Fig. 1(b). A constant bending radius  $R_b$  of 8 cm was adopted in accordance with our experimental conditions. The fiber twisting state  $\gamma$  includes a determined twisting with a peak rate of 5 turn/m and a random twisting with a standard deviation of 0.3 turn/m<sup>1/2</sup> [24]. The simulated relationship between the core pitch and the SMD of CC-4CFs after 1 km propagation is shown in Fig. 1(c) (blue line). The calculated result indicates that the SMD of CC-4CFs is highly dependent on the core pitch. The SMD of the fiber decreases exponentially with the increase of core pitch and the minimum SMD is achieved when the core pitch is about 20  $\mu\text{m}$ . When the core pitch increases further, the SMD increases and gradually converges to a constant value.

We designed and fabricated a group of four-core fibers (4CFs) with different core pitches as shown in Fig. 2 according to the theoretical result. The core pitches were measured to be about

TABLE I  
OPTICAL CHARACTERISTICS OF THE FABRICATED 4CFS

	4CF17	4CF19	4CF20	4CF23	4CF35
Core pitch ( $\mu\text{m}$ )	17	19	20	23	35
Coupling coefficient $\kappa$ ( $\text{m}^{-1}$ )*	86.3	40.1	27.4	8.8	0.1
Attenuation ( $\text{dB/km}$ )	0.25	0.29	0.34	0.21	0.22
Chromatic dispersion ( $\text{ps/nm/km}$ )	17.10	18.74	18.99	16.83	17.72

\* The calculated coupling coefficient between the adjacent cores.

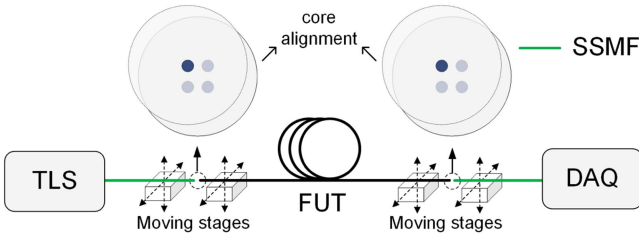


Fig. 3. Experimental setup for SMD measurement.

17, 19, 20, 23, and 35  $\mu\text{m}$ , respectively. These 4CFs are labeled according to their core pitches, namely 4CF17, 4CF19, 4CF20, 4CF23 and 4CF35, respectively. Four cores are arranged in a square lattice structure. Each core of the 4CFs was identical and designed to be a single-mode core in accordance with ITU-T recommendation G.652.D. The core diameter of the fibers was 9  $\mu\text{m}$  with a mode field diameter of about 9.6  $\mu\text{m}$  at 1550 nm.

The attenuations of the fabricated 4CFs were measured with a cutback method [25]. A large-area photodetector was used to receive the output power of all cores when the light was input into a single core in the attenuation measurement. The measured attenuation differences between each input core were lower than 0.1 dB. The attenuations were averaged over each input core and were measured to be about 0.25, 0.29, 0.34, 0.21, and 0.22 dB/km at 1550 nm for 4CFs with core pitch of about 17, 19, 20, 23, and 35  $\mu\text{m}$ , respectively.

The chromatic dispersions (CDs) of each fiber were measured with a phase shift technique [25]. The measured CDs of different 4CFs are listed in Table I. The CDs of fabricated 4CFs were close to the CD of the SSMF.

### III. SPATIAL MODE DISPERSION MEASUREMENT

We measured the SMD of the 4CFs based on the fixed analyzer method, which is usually used in the polarization mode dispersion measurement [26], as shown in Fig. 3. A tunable laser source (TLS) was used to generate the wavelength-scanning signal. Two pairs of moving stages were used to align the input and output SSMF to the same core of the 4CFs. The fibers were wound on the standard 8 cm-radius bobbins. The transmitted spectrum of each core from 1520 nm to 1580 nm with 1 pm step was measured for  $\Lambda = 17, 19, 20,$  and 23  $\mu\text{m}$ . For  $\Lambda = 35 \mu\text{m}$ , the input SSMF was replaced by a 62.5  $\mu\text{m}$ -core MMF. And the MMF

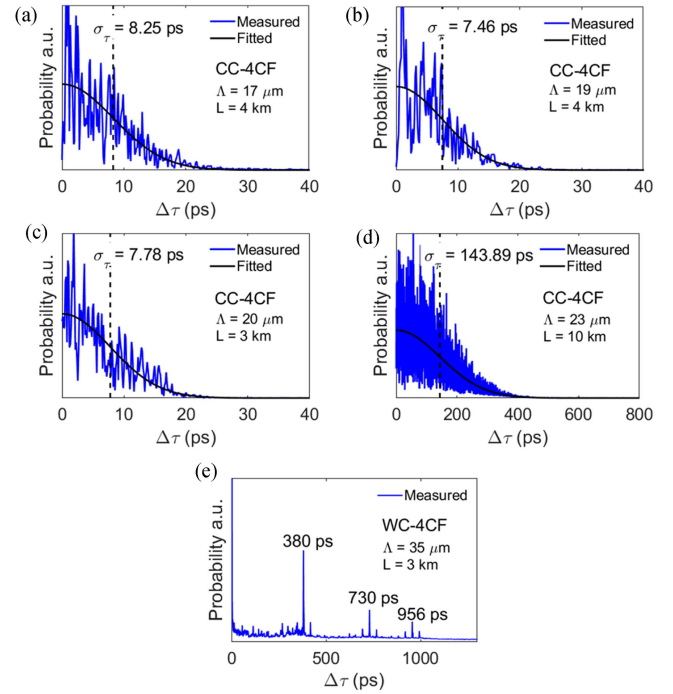


Fig. 4. Measured DGD distribution (blue line) and fitted Gaussian distribution (black line in (a–d)) of the 4CFs.

was directly coupled to the 4CF with center alignment to excite all the spatial modes. The wavelength was set to 1545–1555 nm with 0.1 pm step, and a MMF was used to receive the power from all the output cores.

The measured transmitted spectrum was then Fourier transformed to obtain the autocorrelation function of the intensity impulse response of each fiber, which was also the DGD distribution of the spatial modes. Fig. 4(a)–(d) show the measured DGD distributions of the 4CFs with core pitches of about 17, 19, 20, and 23  $\mu\text{m}$ , respectively. The result was the DGD distribution measured from one core of each fiber, and the DGD distributions of other cores are similar. The DGD distributions were Gaussian shaped due to the random coupling of spatial modes, which indicated that these fibers are CC-4CFs. Fig. 4(e) shows the measured DGD distribution of 4CF with a core pitch of 35  $\mu\text{m}$ . A waveform of several separated peaks was observed, indicating a negligible coupling between the core of this fiber. As a result, the fiber with core pitch of 35  $\mu\text{m}$  is a WC-4CF at a length of 3 km. The delays of these peaks in Fig. 4(e) were time delays between the light propagating independently in different cores, which might be introduced by the core deviation caused by the fabrication process and the existing of fiber bending and twisting.

For CC-4CFs, SMD is defined as the standard deviation of the Gaussian fit curve for the DGD distribution. The measured SMD coefficient was averaged over the result of four cores, as listed in Table II. We compared the measured SMD coefficients with the simulated ones, as shown in Fig. 1(c) red squares and blue lines. The experimental results agreed well with the simulated ones. The SMD coefficients can be well suppressed



TABLE II  
MEASURED SMD COEFFICIENT OF THE CC-4CFs [ps/km<sup>1/2</sup>]\*

	Core1	Core2	Core3	Core4	Avg.
$\Lambda=17\ \mu\text{m}$	4.27	4.08	4.34	4.13	4.21
$\Lambda=19\ \mu\text{m}$	3.74	3.73	3.70	3.72	3.72
$\Lambda=20\ \mu\text{m}$	4.44	4.90	4.51	4.39	4.56
$\Lambda=23\ \mu\text{m}$	45.5	44.4	45.0	44.0	44.7

\* The bending radius of the fibers are 8 cm.

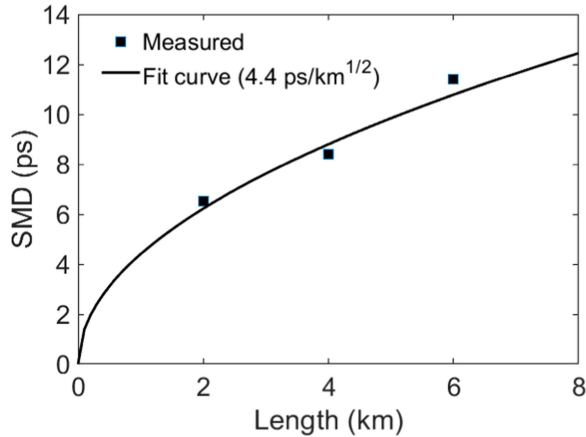


Fig. 5. Dependence of the measured SMD of CC-4CF on fiber length. The fitted curve is calculated to be  $4.4\ \text{ps}/\text{km}^{1/2}$ .

for fibers with a core pitch of around  $20\ \mu\text{m}$ . The measured lowest SMD coefficient of  $3.72\ \text{ps}/\text{km}^{1/2}$  was achieved for a 4 km-long CC-4CF with core pitch of  $19\ \mu\text{m}$ , which is the lowest SMD ever reported when fibers under test were wound on the standard 8 cm-radius bobbins. The difference in the core pitch of the minimum SMD of about  $1\ \mu\text{m}$  between experimental and theoretical results may result from the discrepancy in both fiber fabrication and fiber winding conditions.

The dependence of the SMD of CC-4CF on fiber length was investigated, as shown in Fig. 5. The CC-4CFs with different lengths and core pitch of  $17\ \mu\text{m}$  were both wound on the 8 cm-radius bobbins. The measured SMDs (black squares) fitted well with the black line, which is proportional to the square root of the propagation distance.

#### IV. CHARACTERISTICS OF TRANSFER MATRIX

The transfer matrices of different 4CFs and the matched fan-in and fan-outs (FIFOs) were measured using SWI, which has been commonly used to characterize space-division-multiplexing components and systems [27], [28]. The experiment setup is shown in Fig. 6. The light from the TLS was swept from 1500 to 1600 nm with a sweep rate of 200 nm/s. The main interferometer consisted of the fiber under test (FUT) and a reference SMF. The optical path length of the reference SMF was set to be close to the FUT. The interference fringes between the signals of the FUT and the SMF were obtained with balanced photodetectors (BPD). The transmission spectrum  $H(\omega)$  of the FUT can be extracted from the interference signal. By performing the inverse

Fourier transform on  $H(\omega)$ , the impulse response  $h(t)$  can be obtained. The auxiliary interferometer structure in the lower part of Fig. 6 was used to compensate for the phase noise of the swept-wavelength laser [29].

Two orthogonal polarization states were input into the 4CFs through a polarization multiplexer placed in front of the  $1\times 4$  splitter. The two input polarizations were delayed ( $\tau_7$ ) with each other to ensure that signals with different input polarization states do not mix in the beat frequency domain. The output signal of two polarization states was received separately through a polarization beam splitter (PBS). Considering two orthogonal polarizations of each spatial mode, the 4CFs systems include 8 inputs and 8 outputs corresponding to an  $8\times 8$  transfer matrix.

For CC-4CFs, the 64 elements of the full  $8\times 8$  complex transfer matrix need to be measured together due to the strong coupling between the spatial modes. By adding different fiber delays ( $\tau_1-\tau_6$ ) in the front and the end of the FUT, the impulse responses of each input-output combination were time interleaved by 1 ns so that all the elements in the  $8\times 8$  impulse responses matrix can be simultaneously obtained. The measured intensity impulse response matrices of the CC-4CFs with core pitch of 17, 19, and  $23\ \mu\text{m}$  were shown in Figs. 7–9. The lengths of the fibers were 4 km, 4 km, and 10 km, respectively. Here, the full  $8\times 8$  matrix was reduced to a  $4\times 4$  intensity impulse response matrix, in which the polarizations of each spatial mode were summed together. The second-order dispersion was numerically compensated during the signal process. In Figs. 7–9, the measured impulse responses of different CC-4CFs are both Gaussian-shaped and the  $8\times 8$  impulse response waveforms in each matrix are found to be almost identical. These results indicate that the spatial modes were strongly coupled in these fibers. The pulse widths (twice the standard deviation of the Gaussian-fitted impulse response) were averaged over different inputs and outputs and were measured to be 8.38, 7.85, and 147.47 ps for CC-4CFs with core pitch of 17, 19, and  $23\ \mu\text{m}$ . The corresponding SMD coefficients are 4.19, 3.96, and  $46.63\ \text{ps}/\text{km}^{1/2}$ , respectively. The impulse responses of CC-4CFs are highly dependent on the core pitch, and the optimal value is consistent to our simulation result.

The spectral transfer matrix can be obtained by performing Fourier transform on each element of the  $8\times 8$  impulse response matrix (both the spatial modes and polarizations are considered). The MDL can be calculated by performing singular value decomposition (SVD) on the  $8\times 8$  spectral transfer matrix at each optical frequency. The MDL value is the ratio between the maximum and the minimum  $\lambda_i^2(\omega)$ , where the  $\lambda_i(\omega)$  are the singular values [30]. Fig. 10 shows the estimated MDLs for different CC-4CFs over the 100 nm bandwidth. All the MDLs were lower than 6 dB over the entire 100 nm bandwidth. For CC-4CF with core pitch of  $19\ \mu\text{m}$ , the MDL was relatively flat and below 3 dB within the whole measurement range. The MDL we estimated included the loss difference between cores of the CC-4CFs and the FIFOs with corresponding core pitches. Table III lists the insertion losses of the FIFOs used in the experiment, which were designed and fabricated by fused tapering method [31]. The deviation of different FIFO ports for core pitch of  $17\ \mu\text{m}$  was relatively higher than the others. Therefore, we observed higher MDL levels and more fluctuations in the measured result

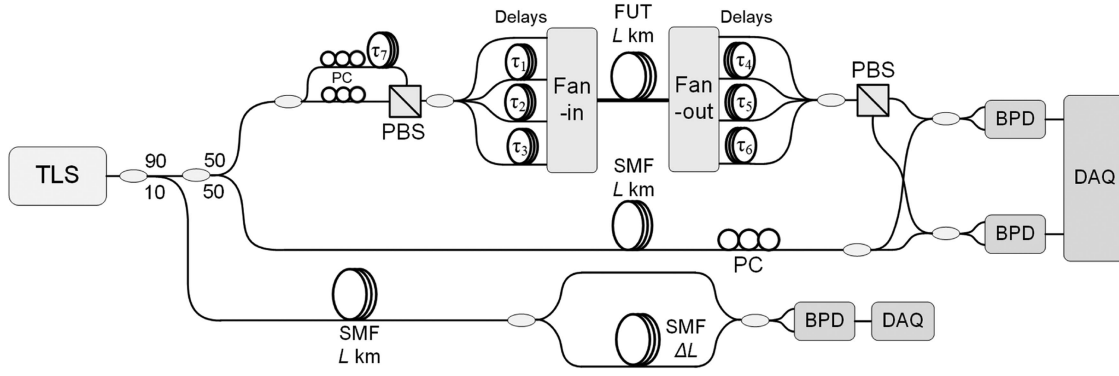
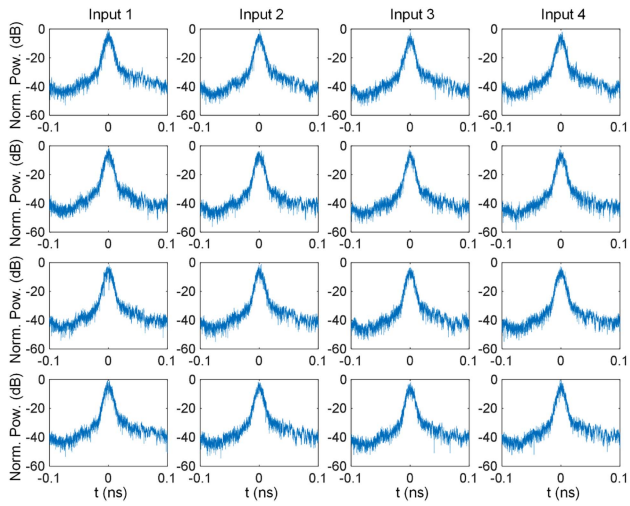
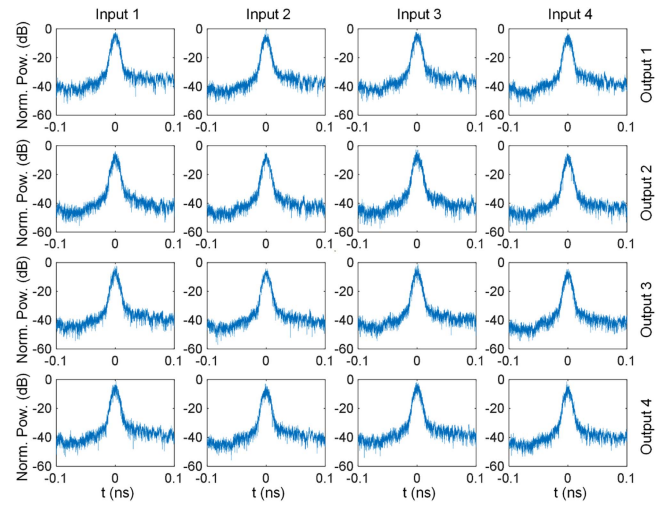


Fig. 6. Experiment setup of swept-wavelength interferometry.

Fig. 7. Measured impulse response for 4 km-long CC-4CF with  $\Lambda = 17 \mu\text{m}$ .Fig. 8. Measured impulse response for 4 km-long CC-4CF with  $\Lambda = 19 \mu\text{m}$ .TABLE III  
MEASURED INSERTION LOSS OF FIFO FOR DIFFERENT FIBERS [dB]

		Port1	Port2	Port3	Port4
$\Lambda=17 \mu\text{m}$	Fan-in	1.89	1.42	1.03	1.39
	Fan-out	2.66	2.32	2.89	1.24
$\Lambda=19 \mu\text{m}$	Fan-in	1.78	1.01	1.43	1.76
	Fan-out	1.00	0.77	1.31	1.00
$\Lambda=23 \mu\text{m}$	Fan-in	1.65	2.03	1.36	1.62
	Fan-out	1.05	1.14	1.95	1.61
$\Lambda=35 \mu\text{m}$	Fan-in	0.51	1.29	1.21	1.69
	Fan-out	0.77	0.99	1.04	1.20

for the CC-4CF with core pitch of  $17 \mu\text{m}$ . Fig. 10(c) shows the estimated MDL for CC-4CF with core pitch of  $23 \mu\text{m}$ . There was a slight increase of the MDL in the short wavelength region, which may be induced by the wavelength dependence of the FIFO device. For CC-4CF with core pitch of both  $17$  and  $23 \mu\text{m}$ , the MDL was lower than  $6 \text{ dB}$  over the  $100 \text{ nm}$  bandwidth.

We also measured the impulse response matrix of the WC-4CF with core pitch of  $35 \mu\text{m}$  (4CF35). Fig. 11 shows the

measured impulse response matrix of a  $5 \text{ m}$ -long 4CF35 and FIFO. It can be found that the light incident from each core was still transmitted in the same core without distortion. The small pulses in the non-diagonal items of the impulse response matrix were induced by the crosstalk of the FIFO device and were smaller than  $-40 \text{ dB}$ . The impulse response matrix for the  $3 \text{ km}$ -long 4CF35 and the FIFO was measured, as shown in Fig. 12. The light mainly propagated within the input core. But the pulses would broaden due to the inter-core crosstalk during the propagation. In the impulse response matrix, the pulse tails in the diagonal term and the plateaus in the non-diagonal term corresponded to the crosstalk from the incident core to the other cores. The plateau width in the non-diagonal term was the group delay difference (or inter-core skew) between the corresponding input and output cores. The relative group delays of the  $3 \text{ km}$ -long 4CF35 were estimated to be  $0, 1.00, -0.69,$  and  $-0.38 \text{ ns}$  for core 1, 2, 3, and 4, respectively. The results agree well with the result in Fig. 4(e). The integrals of the crosstalk plateau were the relative crosstalk level between the corresponding input and output cores, which was measured to be lower than  $-15 \text{ dB}$ . The crosstalk of the 4CF35 was relatively high since the index profile

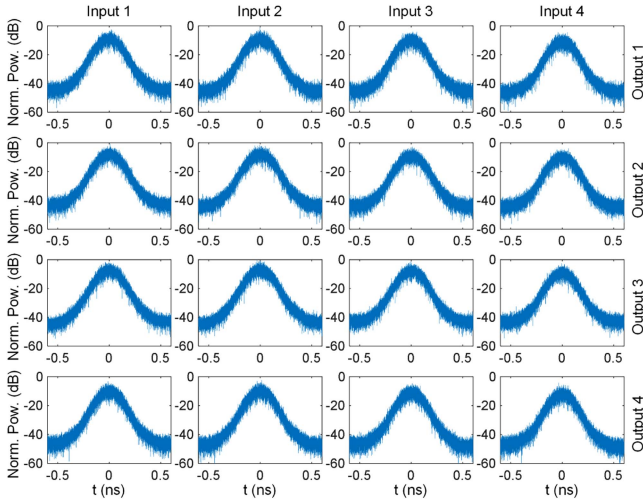


Fig. 9. Measured impulse response for 10 km-long CC-4CF with  $\Lambda = 23 \mu\text{m}$ .

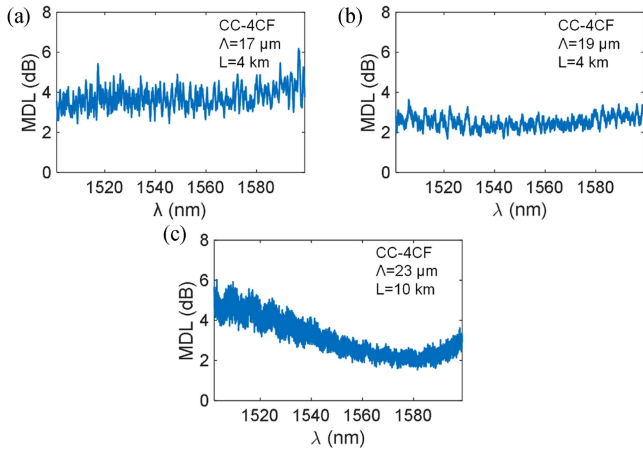


Fig. 10. Estimated MDL for (a) 4 km-long CC-4CF with  $\Lambda = 17 \mu\text{m}$ , (b) 4 km-long CC-4CF  $\Lambda = 19 \mu\text{m}$  and (c) 10 km-long CC-4CF with  $\Lambda = 23 \mu\text{m}$ .

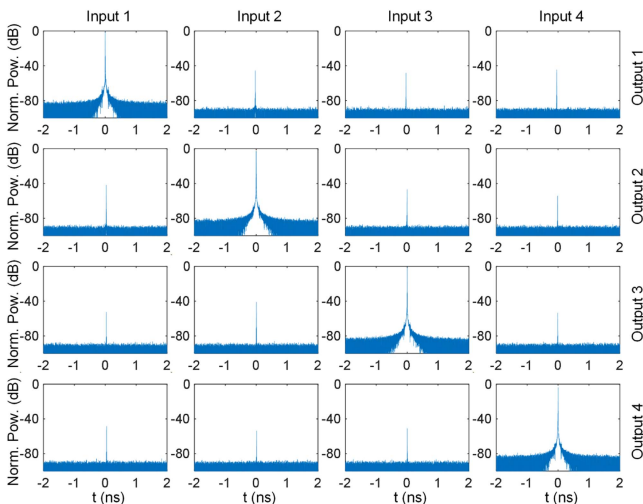


Fig. 11. Measured impulse response for 5 m-long WC-4CF with  $\Lambda = 35 \mu\text{m}$ .

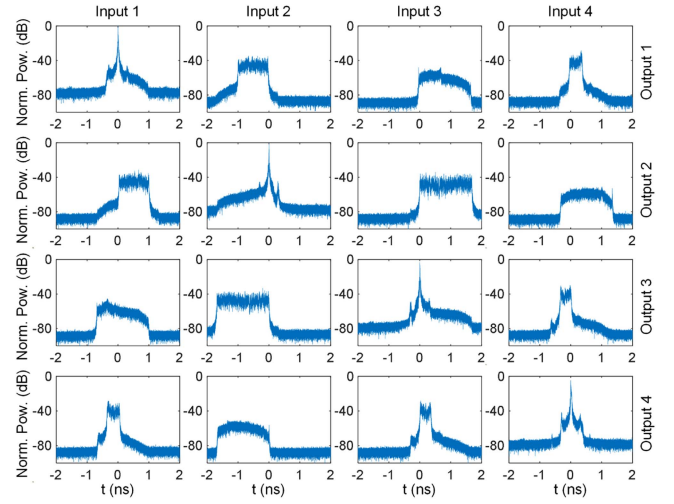


Fig. 12. Measured impulse response for 3 km-long WC-4CF with  $\Lambda = 35 \mu\text{m}$ .

of the fiber is a step-index structure to maintain consistency with other fibers in our experiments. Various structures like trench-assisted and air-hole-assisted designs can be used to reduce the crosstalk in the design of weakly-coupled multicore fibers.

## V. CONCLUSION

We studied the characteristics of coupled-core four-core fibers (CC-4CFs) with different core pitches both theoretically and experimentally. The spatial mode dispersions of different fibers were analyzed, and the result agrees well with theoretical ones. In the experiment, we achieved a spatial mode dispersion as low as  $3.72 \text{ ps/km}^{1/2}$  with core pitch of  $19 \mu\text{m}$  at a bending radius of 8 cm. The impulse response matrices of different fibers were measured using the SWI method. For CC-4CFs, the impulse responses are Gaussian-shaped and almost consistent between different inputs and outputs. The CC-4CFs with core pitches of 17 and  $19 \mu\text{m}$  shown narrower pulse broadening. We calculated the averaged pulse width and MDL of different CC-4CFs from the measured impulse response matrices. The averaged pulse widths agree well with the measured SMD. The dependence of MDL on core pitch was discussed. For CC-4CF with core pitch of  $19 \mu\text{m}$ , the estimated MDL is lower than 3 dB for the entire 100 nm bandwidth. The presented studies give a detailed investigation for the impact of the core pitch on the performance of multicore fibers and are beneficial for developing coupled-core multicore fibers for long-haul transmission applications.

## ACKNOWLEDGMENT

The authors thank Mr. Linbin Bai of Shanghai Optoweave Technology, Co., Ltd. for his advice and help on FIFO device fabrication.

## REFERENCES

- [1] R. - J. Essiambre, G. Kramer, P. J. Winzer, G. J. Foschini, and B. Goebel, "Capacity limits of optical fiber networks," *J. Lightw. Technol.*, vol. 28, no. 4, pp. 662–701, Feb. 2010.
- [2] B. J. Puttnam, G. Rademacher, and R. S. Luís, "Space-division multiplexing for optical fiber communications," *Optica*, vol. 8, no. 9, pp. 1186–1203, 2021.
- [3] D. J. Richardson, J. M. Fini, and L. E. Nelson, "Space-division multiplexing in optical fibres," *Nature Photon.*, vol. 7, no. 5, pp. 354–362, 2013.
- [4] T. Matsui, P. L. Pondillo, and K. Nakajima, "Weakly coupled multicore fiber technology, deployment, and systems," *Proc. IEEE*, vol. 110, no. 11, pp. 1772–1785, Nov. 2022.
- [5] T. Hayashi et al., "Coupled-core multi-core fibers: High-spatial-density optical transmission fibers with low differential modal properties," in *Proc. IEEE Eur. Conf. Opt. Commun.*, 2015, pp. 1–3.
- [6] K. - P. Ho and J. M. Kahn, "Mode-dependent loss and gain: Statistics and effect on mode-division multiplexing," *Opt. Exp.*, vol. 19, no. 17, pp. 16612–16635, 2011.
- [7] R. Ryf, N. K. Fontaine, H. Chen, and R. - J. Essiambre, "Coupled-core fibers: Where mode scrambling mitigates nonlinear effects," in *Proc. Photonic Netw. Devices*, 2017, Art. no. NeTh2B.2.
- [8] M. Arikawa, K. Nakamura, K. Hosokawa, and K. Hayashi, "Long-haul WDM/SDM transmission over coupled 4-core fiber with coupled 4-core EDFA and its mode dependent loss characteristics estimation," *J. Lightw. Technol.*, vol. 40, no. 6, pp. 1664–1671, Mar. 2022.
- [9] S. Beppu et al., "Long-haul coupled 4-core fiber transmission over 7,200 km with real-time MIMO DSP," *J. Lightw. Technol.*, vol. 40, no. 6, pp. 1640–1649, Mar. 2022.
- [10] L. Sun et al., "Theoretical investigations of weakly-and strongly-coupled multi-core fibers for the applications of optical submarine communications under power and fiber count limits," *Opt. Exp.*, vol. 31, no. 3, pp. 4615–4629, 2023.
- [11] S. Ö. Arik, D. Askarov, and J. M. Kahn, "Effect of mode coupling on signal processing complexity in mode-division multiplexing," *J. Lightw. Technol.*, vol. 31, no. 3, pp. 423–431, Feb. 2012.
- [12] P. J. Winzer and G. J. Foschini, "MIMO capacities and outage probabilities in spatially multiplexed optical transport systems," *Opt. Exp.*, vol. 19, no. 17, pp. 16680–16696, 2011.
- [13] T. Sakamoto, T. Mori, M. Wada, T. Yamamoto, F. Yamamoto, and K. Nakajima, "Fiber twisting-and bending-induced adiabatic/nonadiabatic super-mode transition in coupled multicore fiber," *J. Lightw. Technol.*, vol. 34, no. 4, pp. 1228–1237, Feb. 2016.
- [14] T. Hayashi et al., "Randomly-coupled multi-core fiber technology," *Proc. IEEE*, vol. 110, no. 11, pp. 1786–1803, Nov. 2022.
- [15] T. Hayashi et al., "Effects of core count/layout and twisting condition on spatial mode dispersion in coupled multi-core fibers," in *Proc. IEEE 42nd Eur. Conf. Opt. Commun.*, 2016, pp. 1–3.
- [16] M. Mazur et al., "Real-time MIMO transmission over field-deployed coupled-core multi-core fibers," in *Proc. Opt. Fiber Commun. Conf.*, 2022, Art. no. Th4B.8.
- [17] K. Saitoh, T. Fujisawa, and T. Sato, "Control of group delay spread in randomly-coupled multicore fibers," in *Proc. IEEE Opto-Electron. Commun. Conf.*, 2020, pp. 1–3.
- [18] M. Uyama et al., "Bandwidth-decomposed analysis of spatial-mode dispersion of coupled 2-core fiber employing linear optical sampling," *J. Lightw. Technol.*, vol. 41, no. 10, pp. 3153–3163, May 2023.
- [19] M. Mazur et al., "Transfer matrix characterization of field-deployed MCFs," in *Proc. IEEE Eur. Conf. Opt. Commun.*, 2020, pp. 1–4.
- [20] K. Saitoh, "Multi-core fiber technology for SDM: Coupling mechanisms and design," *J. Lightw. Technol.*, vol. 40, no. 5, pp. 1527–1543, Mar. 2022.
- [21] M. B. Shemirani, W. Mao, R. A. Panicker, and J. M. Kahn, "Principal modes in graded-index multimode fiber in presence of spatial- and polarization-mode coupling," *J. Lightw. Technol.*, vol. 27, no. 10, pp. 1248–1261, May 2009.
- [22] K. Okamoto, *Fundamentals of Optical Waveguides*. Amsterdam, The Netherlands: Elsevier, 2006.
- [23] S. Fan and J. M. Kahn, "Principal modes in multimode waveguides," *Opt. Lett.*, vol. 30, no. 2, pp. 135–137, 2005.
- [24] T. Hayashi, Y. Tamura, T. Hasegawa, and T. Taru, "Record-low spatial mode dispersion and ultra-low loss coupled multi-core fiber for ultra-long-haul transmission," *J. Lightw. Technol.*, vol. 35, no. 3, pp. 450–457, Feb. 2016.
- [25] "Definitions and Test Methods for Linear, Deterministic Attributes of Single-Mode Fibre and Cable," ITU-T Recommendation G.650.1, Geneva, Switzerland: International Telecommunications Union, 2010.
- [26] N. Gisin, R. Passy, and J. - P. Von der Weid, "Definitions and measurements of polarization mode dispersion: Interferometric versus fixed analyzer methods," *IEEE Photon. Technol. Lett.*, vol. 6, no. 6, pp. 730–732, Jun. 1994.
- [27] N. K. Fontaine, "Characterization of space-division multiplexing fibers using swept-wavelength interferometry," in *Proc. IEEE Opt. Fiber Commun. Conf.*, 2015, pp. 1–3.
- [28] M. Mazur et al., "Transfer matrix characterization and mode-dependent loss optimization of packaged 7-core coupled-core EDFA," in *Proc. IEEE Eur. Conf. Opt. Commun.*, 2021, pp. 1–4.
- [29] X. Fan, Y. Koshikiya, and F. Ito, "Phase-noise-compensated optical frequency-domain reflectometry," *IEEE J. Quantum Electron.*, vol. 45, no. 6, pp. 594–602, Jun. 2009.
- [30] S. Rommel et al., "Few-mode fiber, splice and SDM component characterization by spatially-diverse optical vector network analysis," *Opt. Exp.*, vol. 25, no. 19, pp. 22347–22361, 2017.
- [31] J. Xiong, L. Ma, Y. Shi, L. Bai, and Z. He, "Low loss ultra-small core pitch all-fiber Fan-In/Fan-Out device for coupled-core multicore fibers," *IEEE Photon. J.*, vol. 14, no. 4, Aug. 2022, Art. no. 7146805.